

SOLAR NEUTRINO RATES, SPECTRUM, AND ITS MOMENTS : AN MSW ANALYSIS IN THE LIGHT OF SUPER-KAMIOKANDE RESULTS

Srubabati Goswami^{a 1}, Debasish Majumdar^{b 2}, and Amitava Raychaudhuri^{b 3}

^aSaha Institute of Nuclear Physics,

1/AF Bidhannagar, Calcutta 700 064, India

^bDepartment of Physics, University of Calcutta,

92 Acharya Prafulla Chandra Road, Calcutta 700 009, India

ABSTRACT

We re-examine MSW solutions of the solar neutrino problem taking (a) the results on total rates and the electron energy spectrum from the 825 day SuperKamiokande (SK) data, (b) those on total rates from the Chlorine and Gallium experiments, and (c) moments of the SK electron spectrum. A salient feature of our analysis is the inclusion of the correlations between the theory errors in the global-fit using the data on the total rates and SK electron energy spectrum. Best fit values for the mixing angle and mass splitting are found for oscillations to sequential and sterile neutrinos and the 90% C.L. allowed regions are determined.

PACS Nos.: 14.60.Pq, 26.65.+t, 12.15.Ff

¹E-mail address: sruba@tnp.saha.ernet.in

²E-mail address: debasish@tnpdec.saha.ernet.in

³E-mail address: amitava@cubmb.ernet.in

1 Introduction

There is now strong evidence in support of an oscillatory behavior of neutrinos. The results on atmospheric neutrinos from SuperKamiokande [1] find a comprehensive explanation in terms of oscillations, indicating a non-zero neutrino mass. This result and the long-standing solar neutrino problem have created much excitement in the community.

In this paper we examine the latest solar neutrino data from SuperKamiokande [2] along with those from the radiochemical Chlorine and Gallium experiments assuming that MSW resonant flavor conversion [3] is operative. The above experiments have presented the measured arrival rates [4] which, in all the cases, are less than the predictions from the Standard Solar Model (SSM). In addition, SuperKamiokande (SK) has provided the observed electron energy distribution [5]. We use these data to test the consistency of the MSW mechanism taken together with the SSM predictions. There are several recent MSW analyses of the SK solar neutrino data. These include the two-flavor analysis by the SK group [2], analyses of the 504 day data [6], 708 day data [7], and 825 day data [8], a three-flavor analysis of the 825 day data [9] and an analysis of the same data in a four neutrino framework [10]. Although the general procedure of data fitting adopted is to minimize a χ^2 function, the details of the statistical procedure used vary among the different groups. In this work we indicate two different ways of performing the statistical analysis for the spectrum and the combined rate and spectrum data and check the consistency of the best-fit values of the mass squared differences and the mixing angles obtained. For the analysis of the spectrum results we explore the possibility of using its moments as variables for fitting the data. The main advantage of these moments is that they probe the shape of the spectrum in a manner independent of the ^8B flux normalization uncertainties. For the combined analysis of the rates and the spectrum, apart from the standard procedure of varying the ^8B flux normalization and treating these two sets of data as independent, we also adopt a second method which takes into account the correlations among the rates and the spectrum data.

In addition to the best-fit values of the oscillation parameters we also present the 90% C.L. allowed regions⁴ and the goodness of fit (g.o.f) of a particular solution. The definition of 90% C.L. allowed region used is $\chi^2 \leq \chi_{min}^2 + 4.61$ (6.25) for 2 (3) parameters. By g.o.f. we mean the probability that the χ^2 will exceed χ_{min}^2 . When presenting the allowed region we take χ_{min}^2 to be the value at the *local* minimum in that region, unless otherwise mentioned. This method is also adopted in [10, 8]. The other approach is to present the allowed regions with respect to the global minimum [6, 7]. For the neutrino fluxes and the neutrino production positions within the sun we use the BP98 solar model [11]. We consider the two alternatives of oscillation of the ν_e to a sequential (ν_μ or ν_τ) or a sterile neutrino.

This paper is organized as follows. In the next section we present the formulae for MSW resonant conversion of neutrinos. In section 3 we use the data on the total solar neutrino rates as measured at the Chlorine, Gallium, and SuperKamiokande (825 day data) detectors to obtain the best-fit values of the neutrino mass splitting and the mixing angles. In section 4 we consider the electron energy spectrum observed at SuperKamiokande. We fit the spectrum to the MSW predictions and obtain the best-fit values. We also calculate the normalized moments of this observed spectrum. These variables probe the distortion of the spectrum, independent of the uncertainties of the absolute normalization of the ^8B neutrino spectrum. We also obtain, in this section, the best-fit values of the parameters using the moments. In section 5 we use both the total rates data and the SK electron energy spectrum data to make a combined fit. Here we use two different methods. In the first method we allow the normalization of the ^8B spectrum to vary. In the other approach, we use the SSM prediction for this normalization which allows us to include the correlations between the total rates and the observed spectrum due to astrophysical uncertainties. We end in section 7 with a summary, discussions and conclusions.

⁴Excepting that when we fit the electron energy spectrum data, we present the 95% C.L. allowed regions.

2 Oscillation Probability

In this work we restrict ourselves to the simplest case of mixing between two neutrino flavors. The expression for the probability used is

$$P_{ee}(E_\nu) = 0.5 + [0.5 - \Theta(E_\nu - E_A)X]\cos 2\theta_M \cos 2\theta \quad (1)$$

where Θ is the Heaviside function. θ is the mixing angle in vacuum and θ_M is the mixing angle in matter given by,

$$\tan 2\theta_M = \frac{\Delta m^2 \sin 2\theta}{\Delta m^2 \cos 2\theta - 2\sqrt{2}G_F n_e E_\nu} \quad (2)$$

here n_e is the ambient electron density, E_ν the neutrino energy, and Δm^2 ($= m_2^2 - m_1^2$) the mass squared difference in vacuum.

$$E_A = \Delta m^2 \cos 2\theta / 2\sqrt{2}G_F n_e|_{pr}$$

gives the minimum ν_e energy that can encounter a resonance inside the sun, $n_e|_{pr}$ being the electron density at the point of production. X is the jump-probability between the mass eigenstates and for an approximately exponential density profile, as is the case in the sun, it is given by [12]

$$X = \frac{\exp[-\pi\gamma_R(1 - \cos 2\theta)] - \exp[-2\pi\gamma_R]}{1 - \exp[-2\pi\gamma_R]} \quad (3)$$

where $\gamma_R = \gamma \cos 2\theta / \sin^2 2\theta$ and

$$\gamma = \frac{\pi}{4} \frac{\Delta m^2 \sin^2 2\theta}{E_\nu \cos 2\theta} \frac{1}{\left| \frac{d \ln n_e}{dr} \right|_{res}} \quad (4)$$

3 Observed rates and neutrino oscillations

In this section we perform an MSW analysis of the total rates as measured at the various experiments. The data that we use in our analysis for the total rates are given in Table 1. In particular, we use the 825 day SK data. For the Ga experiments we take the weighted average of the SAGE and Gallex results. Because SK has better statistics we do not include the Kamiokande results.

Experiment	Chlorine	Gallium	SuperKamiokande
$\frac{\text{Observed Rate}}{\text{BP98 Prediction}}$	0.33 ± 0.029	0.57 ± 0.054	0.475 ± 0.015

Table 1: The ratio of the observed solar neutrino rates to the corresponding BP98 SSM predictions used in this analysis. The results are from Refs. [4] and [2]. For Gallium, the weighted average of the SAGE and Gallex results has been used.

We fit the total rates from the three experiments using a standard χ^2 -fitting procedure [13]. The definition of χ^2 used by us is,

$$\chi^2 = \sum_{i,j=1,3} \left(F_i^{th} - F_i^{exp} \right) (\sigma_{ij}^{-2}) \left(F_j^{th} - F_j^{exp} \right) \quad (5)$$

Here $F_i^\xi = T_i^\xi / T_i^{BP98}$ where ξ is *th* (for the theoretical prediction) or *exp* (for the experimental value) and T_i is the total rate in the i -th experiment. F_i^{exp} is taken from Table 1. The error matrix σ_{ij} contains the experimental errors, the theoretical errors and their correlations. For evaluating the error matrix we use the procedure described in [14].

In the presence of neutrino conversions, the detection rate on earth for the radio-chemical experiments ^{37}Cl and ^{71}Ga is predicted to be:

$$T_i^{th} = \sum_{\alpha} \int_{E_{th}} \phi_{\alpha}(E_{\nu}) \sigma_i(E_{\nu}) < P_{ee}(E_{\nu}) >_{\alpha} dE_{\nu} \quad (6)$$

where $\sigma_i(E_{\nu})$ is the neutrino capture cross-section for the i -th detector [15], E_{th} the neutrino threshold energy for detection, and $\phi_{\alpha}(E_{\nu})$ is the neutrino spectrum for the α -th source [15]. The sum is over all the individual neutrino sources. $< P_{ee}(E_{\nu}) >_{\alpha}$ is the neutrino survival probability for the α -th source averaged over the distribution of neutrino production regions in the sun,

$$< P_{ee}(E_{\nu}) >_{\alpha} = \int dr P_{ee}(\Delta m^2, \theta, E_{\nu}, r) \Phi_{\alpha}(r) \quad (7)$$

the dependence on r in P_{ee} coming through the presence of the number density of electrons, n_e , at the position where the neutrino is created. $\Phi_{\alpha}(r)$ is a normalized function of r which gives the probability of the α -th reaction occurring at a distance

r from the center of the sun. The theoretical prediction according to the BP98 solar model, T_i^{BP98} , is obtained by setting the survival probability as 1 in the above.

For SK, in the case of oscillation to sequential neutrinos one has to take into account the contributions to the signal from the produced ν_μ or ν_τ *via* the neutral current interactions,

$$T_{SK}^{th} = \sum_{\alpha} \int_{E_{A_{th}}} dE_A \int_0^{\infty} dE_T \rho(E_A, E_T) \int_{E_{\nu_{min}}}^{E_{\nu_{max}}} dE_{\nu} \phi_{\alpha}(E_{\nu}) \left[< P_{ee}(E_{\nu}) >_{\alpha} \frac{d\sigma_{\nu_e}}{dE_T} + < P_{e\mu}(E_{\nu}) >_{\alpha} \frac{d\sigma_{\nu_{\mu}}}{dE_T} \right] \quad (8)$$

The second term in the bracket is absent if oscillation to sterile neutrinos is under consideration. E_T and E_A denote the true and apparent electron energies respectively. $\rho(E_A, E_T)$ is the energy resolution function for which we use the expression given in [16]. $E_{A_{th}}$ is 6.5 MeV for the calculation of the total rate at SK. $\frac{d\sigma}{dE_T}$ is the differential cross-section for the production of an electron with true relativistic energy E_T and can be calculated from standard electroweak theory.

We summarize our best-fit results for the total rates in Table 2. These fits have 1 degree of freedom (3 experimental data points – 2 parameters). It is clear from this Table that the small mixing angle solution for the sequential neutrino case gives by far the best fit to the total rates data. Since we have not included the earth regeneration effect, we do not find the LOW solution (around $\Delta m^2 \sim 10^{-8}$ eV²) which has been reported to be allowed with a lower g.o.f by some groups [6, 7].

It may be of interest to see how these results compare with those for the 708 day data [17]. For the 708 day data, for sequential neutrinos the best-fit and χ_{min}^2 that we get are: $\Delta m^2 = 5.2 \times 10^{-6}$ eV², $\sin^2 2\theta = 6.30 \times 10^{-3}$ and $\chi_{min}^2 = 0.15$ for the SMA solution. The best-fit values in the LMA region are $\Delta m^2 = 1.8 \times 10^{-5}$ eV², $\sin^2 2\theta = 0.81$, and $\chi_{min}^2 = 4.59$. Thus the best-fit values obtained for the 825 day data are not markedly different from those obtained for the 708 day data. This indicates that the best-fit points obtained from the analysis of total rates are quite robust and are not expected to change drastically with more data from SK.

Type of Neutrino	Nature of Solution	Δm^2 in eV^2	$\sin^2(2\theta)$	χ_{min}^2	Goodness of fit
Sequential	SMA	5.3×10^{-6}	6.05×10^{-3}	0.06	80.64%
	LMA	2.4×10^{-5}	0.86	4.49	3.41%
Sterile	SMA	3.8×10^{-6}	6.30×10^{-3}	1.33	24.88%
	LMA	No solution at 99% C.L.			

Table 2: The best-fit values of the parameters, χ_{min}^2 , and the g.o.f. for fits to the total rates of the different experiments. SMA and LMA stand for the Small Mixing Angle and Large Mixing Angle regions, respectively.

In Figure 1 we show the 90% C.L. contours in the $\sin^2(2\theta) - \Delta m^2$ plane for the MSW solution to sequential and sterile neutrinos. As noted in Table 2, for the latter case there is no solution for the LMA region.

4 Observed spectrum, its moments, and neutrino oscillations

In addition to the total rates, SK has provided the number of events in 17 electron recoil energy bins of width 0.5 MeV in the range 5.5 MeV to 14 MeV and an 18th bin which covers the events in the range 14 to 20 MeV [2, 17].

4.1 Observed spectrum and neutrino oscillations

In this section we analyze the spectral data [2] in the light of the MSW effect. The definition of χ^2 used by us is,

$$\chi^2 = \sum_{i,j=1,18} \left(X_B R_i^{th} - R_i^{exp} \right) (\sigma_{ij}^{-2})_{sp} \left(X_B R_j^{th} - R_j^{exp} \right) \quad (9)$$

where X_B allows for an arbitrary normalization of the ^8B flux with respect to the SSM prediction and $R_i^\xi = S_i^\xi/S_i^{BP98}$ with ξ being *th* or *exp* as before and S_i standing for the number of events in the i -th energy bin. The theoretical prediction is given by eq. (8) but the integration over the apparent (*i.e.*, measured) energy will now be over each bin. The error matrix σ_{ij} used by us is [7]

$$(\sigma_{ij}^2)_{sp} = \delta_{ij}(\sigma_{i,stat}^2 + \sigma_{i,uncorr}^2) + \sigma_{i,exp}\sigma_{j,exp} + \sigma_{i,cal}\sigma_{j,cal} \quad (10)$$

where we have included the statistical error, the uncorrelated systematic errors and the energy-bin-correlated experimental errors [18] as well as those from the calculation of the shape of the expected spectrum [19]. Since we vary the normalization of the ^8B flux we do not include its astrophysical uncertainties separately.

For this analysis we find two regions of minima. One is in the region where X_B , the ^8B normalization (with respect to the SSM value), is ≤ 1.5 . The results for this case are shown in Table 3.

Type of Neutrino	Nature of Solution	Δm^2 in eV^2	$\sin^2(2\theta)$	X_B	χ_{min}^2	Goodness of fit
Sequential	SMA	1.6×10^{-8}	2.0×10^{-3}	0.45	17.62	28.32%
	LMA	1.0×10^{-7}	0.79	1.13	17.66	28.09%
Sterile	SMA	1.6×10^{-8}	$(0.3 - 30) \times 10^{-2}$	0.45-0.47	17.85	27.06%
	LMA	5.0×10^{-8}	0.97	1.09	17.66	28.09%

Table 3: The best-fit values of the parameters, χ_{min}^2 , and the g.o.f for fits to the observed electron energy spectrum from SK (825 days) when the ^8B flux normalization factor X_B is restricted not to exceed 1.5.

For the case of oscillation to a sterile neutrino, there is a range in the parameter space in the SMA region over which the χ^2 assumes its minimum value. From the results of Table 3 it is clear that, unlike the total rates, the electron energy spectrum data do not clearly prefer any one of the four solutions examined.

The SK group had earlier presented electron energy spectra as measured over a span of 708 days. In Table 4 we present the best-fit values of the parameters as obtained by using this data set.

Type of Neutrino	Nature of Solution	Δm^2 in eV^2	$\sin^2(2\theta)$	X_B	χ^2_{min}	Goodness of fit
Sequential	SMA	2.0×10^{-7}	1.4×10^{-2}	0.47	18.16	25.43%
	LMA	1.0×10^{-7}	0.73	1.15	17.86	27.01%
Sterile	SMA	2.0×10^{-7}	0.01	0.47	18.17	25.38%
	LMA	8.4×10^{-8}	0.90	1.24	17.97	26.42%

Table 4: The best-fit values of the parameters, χ^2_{min} , and the g.o.f for fits to the observed electron energy spectrum from the 708 day SK data when the ^8B flux normalization factor X_B is restricted not to exceed 1.5.

Though the results of Tables 3 (825 day data) and 4 (708 day data) are broadly similar, the larger sample favours a slightly smaller Δm^2 in the SMA region.

In addition to the region of minima noted above ($X_B \leq 1.5$), there is another in the region where X_B is > 2.0 . The results for this case are shown in Table 5.

Type of Neutrino	Nature of Solution	Δm^2 in eV^2	$\sin^2(2\theta)$	X_B	χ^2_{min}	Goodness of fit
Sequential	SMA	3.4×10^{-5}	4.0×10^{-3}	2.82	17.13	31.11%
	LMA	1.4×10^{-6}	0.1	2.47	17.25	30.41%
Sterile	SMA	No solution				
	LMA	5.0×10^{-7}	0.35	4.46	17.42	29.44%

Table 5: The best-fit values of the parameters, χ^2_{min} , and the g.o.f. for fits to the electron energy spectrum from SK (825 days) when the ^8B flux normalization factor X_B is larger than 2.

From Tables 3 and 5 we see that the quality of fit in the high X_B region is marginally better than that in the low X_B region.

We present in Figure 2 the 95% C.L. allowed region ($\chi^2 \leq \chi^2_{min} + 7.82$ for 3 parameters) in the $\sin^2(2\theta) - \Delta m^2$ plane from the spectrum data. Several remarks need to be made. The areas *within* the contours are *excluded*. The absolute normalization of the ^8B flux, X_B , is allowed to vary freely. In this plot the 95% χ^2 limits are calculated with respect to the *global minimum*. It is seen from this Figure that a much larger region of parameter space is excluded for the sterile neutrino case. Nevertheless, the present electron energy spectrum data clearly does not put a tight bound on the oscillation parameters.

In Figure 3a (3b) we present the recoil electron energy spectrum obtained using the best-fit values of the parameters in the SMA (LMA) region – for both the low and high X_B cases – for MSW conversion to sequential neutrinos. Fig. 3c exhibits the corresponding results for the sterile neutrino alternative. As noted in Table 5, no solution in the SMA region was obtained with high X_B for sterile neutrinos. It is seen from these figures that in all the cases the solutions with high X_B give spectra which grow at higher energies, leading to a better fit to the data.

4.2 Moments of spectrum and neutrino oscillations

Since the absolute normalization of the ^8B flux is not precisely known, it is of interest to look for variables which probe neutrino oscillation effects in the data in a manner immune to this uncertainty. Normalized moments of the observed electron spectrum can be useful as one such set of variables [20, 21]. These can be defined as:

$$M_n = \frac{\sum_i N(E_i) E_i^n}{\sum_i N(E_i)} \quad (11)$$

where E_i is the mean energy of the i -th bin and N_i is the number of events in this bin. It is clear that these variables carry information about the shape of the neutrino spectrum which, if oscillations are operative, undergoes modification from the SSM prediction due to the energy dependence of the survival probability. It is obvious that

the above moments are independent of the absolute normalization of the ^8B flux.

In practice, to compare with the data, it is convenient to standardize with respect to the SSM predictions by using in place of eq. (11)

$$M_n = \frac{\sum_i \left[\frac{N(E_i)}{\{N(E_i)\}_{SSM}} \right] E_i^n}{\sum_i \left[\frac{N(E_i)}{\{N(E_i)\}_{SSM}} \right]} \quad (12)$$

where depending on whether the experimental or the theoretically predicted value of the variable is under consideration, $N(E_i)$ is obtained either from experiments or from the theoretical model under test. If oscillations are operative, then the moments can be readily calculated from eq. (8). We skip the detailed formula here.

We have calculated the moments of the 825 day data on the electron energy spectrum presented by SuperKamiokande [2]. These are presented in Table 6. The error in the higher moments increases rapidly with the order and the ones beyond the sixth are no longer useful.

Order of Moment	Value of Moment	Calculated Error in Moment
1	10.41	0.84
2	117.41	12.89
3	1420.59	236.81
4	18246.67	4680.06
5	246450.36	93497.84
6	3472050.50	1849185.88

Table 6: Moments of the observed electron energy spectrum and their calculated errors obtained from the SK (825 days) data.

Using these variables in a χ^2 -analysis we find that fitting the first five moments gives the same best-fit values of Δm^2 and $\sin^2(2\theta)$ as those obtained using the first six moments. Our results are shown in Table 7. The small values of χ^2_{min} for these fits

should not be regarded as a major success of the theory but rather reflect the large errors associated with the moments as obtained from the present data.

Type of Neutrino	Nature of Solution	Δm^2 in eV^2	$\sin^2(2\theta)$	χ^2_{min}	Goodness of fit
Sequential	SMA	5.8×10^{-5}	0.97×10^{-3}	0.0043	99.99%
	LMA	0.8×10^{-5}	1.0	0.788	85.23%
Sterile	SMA	6.5×10^{-6}	3.7×10^{-2}	0.0017	99.99%
	LMA	$(0.8 - 21) \times 10^{-5}$	1.0	0.7471	86.21%

Table 7: The best-fit values of the parameters, χ^2_{min} , and the g.o.f. for fits to the first five moments of the observed electron energy spectrum at SK (825 days).

To gauge the impact of the higher moments on the final best-fit values, we present in Table 8 the results obtained by fitting the first three moments only.

Type of Neutrino	Nature of Solution	Δm^2 in eV^2	$\sin^2(2\theta)$	χ^2_{min}	Goodness of fit
Sequential	SMA	6.5×10^{-4}	0.87×10^{-3}	0.0009	97.60%
	LMA	$(0.25 - 1.9) \times 10^{-5}$	1.0	0.537	46.36%
Sterile	SMA	1.9×10^{-6}	1.6×10^{-2}	0.0025	96.01%
	LMA	$(0.4 - 8700) \times 10^{-7}$	1.0	0.507	47.64%

Table 8: The best-fit values of the parameters, χ^2_{min} , and the g.o.f. for fits to the first three moments of the observed electron energy spectrum at SK (825 days).

Comparing Tables 7 and 8, it is seen that though the quality of the fit for the SMA solutions do not change much due to the inclusion of the higher moments, the LMA solutions for both sequential and sterile neutrinos are strongly affected. It is clear from Table 8, that the SMA solution is favoured for both the sequential and sterile neutrino cases. Clearly more data will be of help here.

5 Combined fits to rates and spectrum

In this section we present the results of the combined fit to the total rates and the spectrum data. We have performed this global fit by the following two ways

- (a) We treat the rates and the electron spectrum data as independent. In this approach we vary the ^8B flux normalization as a free parameter.
- (b) We do not vary the ^8B flux normalization as a free parameter but include the correlations of the ^8B flux uncertainty between the rates and spectrum data. This approach has not been pursued in any previous analysis.

5.1 Fits using the ^8B flux normalization as a free parameter

For this case the definition of χ^2 is,

$$\begin{aligned} \chi^2 = & \sum_{i,j=1,3} \left(F_i^{th} - F_i^{exp} \right) (\sigma_{ij}^{-2}) \left(F_j^{th} - F_j^{exp} \right) \\ & + \sum_{i,j=1,18} \left(X_B R_i^{th} - R_i^{exp} \right) (\sigma_{ij}^{-2})_{sp} \left(X_B R_j^{th} - R_j^{exp} \right) \end{aligned} \quad (13)$$

where the first term on the r.h.s is from eq. (5) and the second from eq. (9). As we allow the normalization of the ^8B flux to vary as a free parameter we switch off the astrophysical uncertainties arising because of this component. Since it is the ^8B flux that enters the rates as well as the spectrum data, in this manner of fitting the data the correlations between the rates and the spectrum are absent; the error matrix is block diagonal and one can sum the χ_{rate}^2 and $\chi_{spectrum}^2$ independently. There are 18 ($= 21 - 3$) degrees of freedom in this case. The best-fit values we obtain are presented in Table 9.

The SMA region gives a slightly better fit. Though for the fits to the total rates alone no LMA solution is obtained for the sterile neutrino case, we find a high X_B solution in this region from this combined rate and spectrum fit, reflecting the result that the spectrum data give comparable fits for sequential and sterile neutrinos. However, this minimum is somewhat sensitive to the input values of the parameters.

Type of Neutrino	Nature of Solution	Δm^2 in eV^2	$\sin^2(2\theta)$	X_B	χ^2_{min}	Goodness of fit
Sequential	SMA	5.0×10^{-6}	2.7×10^{-3}	0.65	19.11	38.5%
	LMA	1.8×10^{-5}	0.6	1.07	19.60	35.6%
Sterile	SMA	4.9×10^{-6}	2.2×10^{-3}	0.65	20.14	32.5%
	LMA	7.5×10^{-6}	0.29	5.89	22.07	22.89%

Table 9: The best-fit values of the parameters, χ^2_{min} , and the g.o.f. for fits to the total rates measured at the Cl, Ga, and SK detectors along with the electron energy spectrum from SK (825 days) when the ^8B flux normalization factor X_B is allowed to vary.

In Figure 4a (4b) we show the 90% C.L. allowed regions for the combined analysis of total rates and the observed electron spectrum for MSW conversion to sequential (sterile) neutrinos. The best-fit points in these plots are obtained by varying X_B in addition to Δm^2 and $\sin^2(2\theta)$. X_B is held fixed at its best-fit value when obtaining the contours shown in this figure.

5.2 Fits including correlations between rates and spectrum via ^8B flux

For this case we include the correlations in the theory errors between the rate and the spectrum data. This comes through the ^8B flux, as it enters both data. Since we include the astrophysical uncertainties in the ^8B flux the normalization factor for it is held fixed at the SSM value. Now the individual χ^2 due to the spectrum and the rates cannot be summed independently and the combined χ^2 is defined as,

$$\chi^2 = \sum_{i,j=1,21} \left(F_i^{th} - F_i^{exp} \right) (\sigma_{ij}^{-2}) \left(F_j^{th} - F_j^{exp} \right) \quad (14)$$

where the σ_{ij} is now a 21×21 matrix defined in the following way,

- For $i, j = 1 \dots 3$

$$\sigma_{ij}^2 = (\sigma_{ij}^2)_{th} + (\sigma_{ij}^2)_{exp} \quad (15)$$

where

$$(\sigma_{ij}^2)_{th} = \delta_{ij} \sum_{\alpha=1}^8 R_{\alpha i}^2 (\Delta C_{\alpha i})^2 + \sum_{\alpha, \beta=1}^8 R_{\alpha i} R_{\beta j} \sum_{k=1}^9 a_{\alpha k} a_{\beta k} (\Delta \ln X_k)^2. \quad (16)$$

where the first term is due to the cross-section uncertainties and the second term (σ_{ap}) is due to the astrophysical uncertainties [14]. The off-diagonal elements in the error matrix come through σ_{ap} . $R_{\alpha i}$ denotes the contribution of the α -th source to the rate of the i -th experiment. $a_{\alpha k} = \delta \ln \phi_{\alpha} / \delta \ln X_k$, where $\delta \ln \phi_{\alpha}$ is the error in the α -th component of the spectrum due to the input parameter X_k [11].

- For $i = 4 \dots 21$ and $j = 1 \dots 3$

$$\sigma_{ij}^2 = \sum_{\alpha=1}^8 R_{s_{Bi}} R_{\alpha j} \sum_{k=1}^9 a_{s_{Bk}} a_{\alpha k} (\Delta \ln X_k)^2 \quad (17)$$

- For $i = 1 \dots 3$ and $j = 4 \dots 21$

$$\sigma_{ij}^2 = \sum_{\alpha=1}^8 R_{\alpha i} R_{s_{Bj}} \sum_{k=1}^9 a_{\alpha k} a_{s_{Bk}} (\Delta \ln X_k)^2 \quad (18)$$

- for $i = 4 \dots 21$ and $j = 4 \dots 21$

$$\sigma_{ij}^2 = (\sigma_{ij}^2)_{sp} + R_{s_{Bi}} R_{s_{Bj}} \sum_{k=1}^9 a_{s_{Bk}} a_{s_{Bk}} (\Delta \ln X_k)^2 \quad (19)$$

In this case the number of degrees of freedom is 19 ($= 21 - 2$). The χ_{min}^2 and the best-fit values we obtain are shown in Table 10.

We find that the fits are of poorer quality in this case as compared to the previous one. But the best-fit values are not very different except for the LMA sterile neutrino case.

In Figure 5a (5b) we show the 90% C.L. allowed regions for the combined analysis of total rates and the observed electron spectrum for MSW conversion to sequential (sterile) neutrinos including the correlations between the rates and the spectrum due to the astrophysical uncertainties of the ^8B flux normalization.

Type of Neutrino	Nature of Solution	Δm^2 in eV^2	$\sin^2(2\theta)$	χ^2_{min}	Goodness of fit
Sequential	SMA	5.3×10^{-6}	5.69×10^{-3}	20.50	36.5%
	LMA	2.3×10^{-5}	0.84	23.13	23.2%
Sterile	SMA	5.0×10^{-6}	3.85×10^{-3}	23.01	23.7%
	LMA	2.3×10^{-5}	1.0	30.03	5.14%

Table 10: The best-fit values of the parameters, χ^2_{min} , and the g.o.f. for fits to the total rates measured at the Cl, Ga, and SK detectors along with the electron energy spectrum from SK (825 days). In this case the ^8B flux is chosen as in the SSM and the correlation between the rates and the spectrum due to astrophysical uncertainties is included.

6 Summary, Discussions and Conclusions

In this paper we have performed a detailed χ^2 -analysis of the latest SK solar neutrino data together with the results from the Cl and Ga experiments in terms of two-generation MSW conversions of ν_e to sequential (ν_μ , ν_τ) or sterile neutrinos. We find the best-fit values of the parameters from the total rates measured in the different experiments. We fit the observed electron energy spectrum data in two different ways, exploring for the first time, the use of moments of the energy spectrum in a χ^2 -analysis. The combined fits to the total rates and spectral data are also performed in two different manners. In the first, the ^8B flux normalization is used as a free parameter while in the other the SSM normalization is chosen for it and correlations between the rates and spectral data due to astrophysical uncertainties of the ^8B flux are included.

We find that the two-generation MSW scenario can well explain the data on total rates. The solution in the SMA (Small Mixing Angle) region for the sequential neutrino alternative is much preferred over the other possibilities, *viz.* LMA (Large Mixing Angle) sequential, SMA sterile, and LMA sterile. In fact, no solution is obtained at

the 90% C.L. in the very last case. The best-fit values of the parameters have been presented in Table 2 and the 90% C.L. allowed regions in Fig. 1.

When fitting the SK electron energy spectrum data, we have allowed the absolute normalization of the ^8B flux, X_B , to vary. We find two different sets of best-fit values; one in the region $X_B \leq 1.5$ and the other for $X_B > 2$. The latter provide a slightly better fit (goodness of fit $\sim 30\%$) for both sequential and sterile neutrinos in the SMA as well as the LMA cases. We have checked that the results are not much different from those obtained by fitting the earlier 708 day data. The best-fit values are therefore robust. These results can be found in Tables 3, 4, and 5. The 95% C.L. allowed regions from fits to the electron energy spectrum are shown in Fig. 2. The spectra obtained using the best-fit values are compared with the observed data in Fig. 3.

We have next explored the use of normalized moments of the observed electron energy spectrum to signal MSW resonant flavour conversion. These variables are independent of the absolute normalization of the ^8B flux and probe the effect of oscillations on the spectral shape. This procedure is somewhat handicapped by the large errors on the moments calculated from the present data. Goodness of fits larger than 95% are obtained for the SMA case for both sequential and sterile neutrinos from best-fits to the first three normalized moments. The fits are less good in the LMA region. These results are presented in Tables 7 and 8.

We also perform a combined χ^2 -fit to the rates and the spectrum data. So far such a combined analysis has been done by varying the ^8B flux normalization as a free parameter and treating the two sets of data as independent. We use the latest SK data in an analysis following this method. However, since the ^8B flux enters in both the total rates and the spectrum, the correlations between these, neglected in previous analyses, can be important. One novel feature of our work is a second analysis of the combined rates and spectrum data with the inclusion of these correlations. We find that in this method the quality of the fit is poorer but the best-fit points do not change much. Only for the LMA solution to a sterile neutrino are the best-fits obtained in the two cases quite different. Our results obtained by following the two procedures appear

in Tables 9 and 10. The 90% C.L. allowed regions in parameter space from these fits are shown in Figs. 4 and 5.

In this work we have not included the earth regeneration effect and, for this reason, have not used the data on the measurement of the day-night solar neutrino flux [22].

It is necessary at this point to see how our results compare with other recent analyses in the literature. Such comparisons are fraught with some uncertainties since even for the same live days of SK data there are always minor differences like whether the Kamiokande results are included in the fits, whether the Gallex and the SAGE results are used as two different data points or as a weighted average, the treatment of error correlations *etc.* Therefore, such comparisons should be treated with caution. But it may be expected that the best-fit points should not change drastically due to these differences.

Apart from the analysis by the SK group there are two other recent analyses [6, 7] which have presented results separately for the rates, spectrum, as well as rate and spectrum in addition to the results for the global fit to rate, spectrum and zenith angle dependence of the data⁵.

In terms of the number of days of SK data used and treatment of the error correlation in the spectrum analysis our approach is closer to that in [7] which considers the 708 day data. If we compare our results for the 708 day data with the ones obtained there we find that in the SMA sector the two agree very well. The agreement is not as good in the LMA region perhaps because the earth regeneration effect has not been incorporated in our fits. Our analysis of the spectrum data treats the errors in a manner similar to that in Ref. [7]. However, the results in [7] have not been given in such detail for the fits to the spectrum alone and only the global minima for the sequential and the sterile case are reported. We do find a minimum near the best-fit point found in [7] but that is not the global minimum in our analysis (but the two values of χ^2_{min}

⁵In [8] the results for the global fit for the 825 day data are reported but separate results for the spectrum and rate plus spectrum analysis are not given. In [9] the best-fit values are presented for a fit to the total rates, and for the global fit to the rates, spectrum, and day-night asymmetry for the 825 day SK data but the best-fit points for the combined rate plus spectrum analysis is not given.

differ only by 0.7%). However, since the χ^2_{min} in the other regions are not very different from the global minimum, we choose to present all of these. It helps to stress that the spectrum data do not indicate one particular preferred solution. Secondly, the solution in our analysis that matches with the best-fit given in [7] lies in the high X_B region. Since the corresponding X_B is not quoted we cannot compare this aspect. As noted earlier, the high X_B solutions that we get yield a spectrum which increases in the high energy region and fits the data slightly better.

In order to explain the energy spectrum observed at SK, it has been observed that apart from the ^8B flux a *hep* flux almost 20-30 times larger than the SSM prediction can well explain the high energy part of the data [23]. In this work we have not considered this possibility. Whether one requires such a higher *hep* flux compared to the SSM prediction can be tested in SK. However, *we find an important result that from the spectral data alone, a slightly better fit is obtained when the value of the ^8B flux normalization X_B is higher than 2.0 if the hep flux is not included..*

For the combined rate and spectrum analysis, our results agree very well with those in [7]. Since the *hep* flux is also allowed to vary there, this agreement indicates that the best-fit values do not depend sensitively on this aspect though the goodness of fit can differ. A comparison of the last two cases given in Table II of [9] also supports this. We also identify a small allowed zone in the LMA region from the combined rate and spectrum analysis which is not reported elsewhere.

In this work we have varied the mixing angle θ from 0 to $\pi/4$. Recently it has been pointed out [24] that since the MSW probability is not invariant under the transformation $\theta \rightarrow \pi/2 - \theta$ one can get allowed regions beyond $\theta = \pi/4$ (the "dark side"). The effect of varying θ from 0 to $\pi/2$ in the context of the solar neutrino data on the spectrum and zenith angle dependence has been discussed recently in [25].

In conclusion, we have probed the most recent solar neutrino data on total rates and the observed electron energy spectrum at SK from various angles within the framework of MSW flavour conversion. We find good fits in some situations but a degree of uncertainty still remains since different fits do not prefer the same values of the parameters.

More data from the running and new experiments, it is hoped, will further sharpen the results in the near future.

Acknowledgements

D.M. and A.R. are partially supported by the Eastern Centre for Research in Astrophysics, India. A.R. also acknowledges a research grant from the Council of Scientific and Industrial Research, India. We would like to thank Sandhya Choubey for pointing out an error in one of our computer codes. S.G. would like to thank Plamen Krastev for many helpful correspondences.

References

- [1] Y. Fukuda *et al.*, (The Super-Kamiokande collaboration), *Phys. Rev. Lett.* **81**, 1562 (1998).
- [2] Y. Suzuki, Talk given at the Lepton-Photon Symposium '99, <https://www.sldnt.slac.stanford.edu/lp99/db/program.asp>.
- [3] L. Wolfenstein, *Phys. Rev.* **D34**, 969 (1986); S.P. Mikheyev and A.Yu. Smirnov, *Sov. J. Nucl. Phys.* **42(6)**, 913 (1985); *Nuovo Cimento* **9c**, 17 (1986).
- [4] B.T. Cleveland *et al.*, *Nucl. Phys. B (Proc. Suppl.)* **38**, 47 (1995); Y. Fukuda *et al.*, (The Kamiokande collaboration), *Phys. Rev. Lett.* **77**, 1683 (1996); W. Hampel *et al.*, (The Gallex collaboration), *Phys. Lett.* **B388**, 384 (1996); J.N. Abdurashitov *et al.*, (The SAGE collaboration), *Phys. Rev. Lett.* **77**, 4708 (1996).
- [5] Y. Fukuda *et al.*, (The Super-Kamiokande collaboration), *Phys. Rev. Lett.* **81**, 1158 (1998); **82**, 2430 (1999).
- [6] J.N. Bahcall, P.I. Krastev, and A.Yu. Smirnov, *Phys. Rev.* **D58**, 096016 (1998).

- [7] M.C. Gonzalez-Garcia, P.C. de Holanda, C. Peña-Garay, and J.W.F. Valle, hep-ph/9906469.
- [8] J.N. Bahcall, P.L. Krastev, and A.Yu. Smirnov, *Phys. Lett.* **B477**, 401 (2000).
- [9] G.L. Fogli *et al.*, hep-ph/9912231.
- [10] C. Giunti, M.C. Gonzalez-Garcia, and C. Peña-Garay, hep-ph/0001101.
- [11] J.N. Bahcall, S. Basu, and M. Pinsonneault, *Phys. Lett.* **B433**, 1 (1998).
- [12] S.T. Petcov, *Phys. Lett.* **B200**, 373 (1988).
- [13] MINUIT version 92.1, CERN Program Library Long Writeup D506.
- [14] G.L. Fogli and E. Lisi, *Astropart. Phys.* **3**, 185 (1995).
- [15] <http://www.sns.ias.edu/~jnb/SNdata>.
- [16] J.N. Bahcall, E. Lisi, and P.I. Krastev *Phys. Rev.* **C55**, 494 (1997).
- [17] M. Smy, (The Super-Kamiokande collaboration), hep-ex/9903034.
- [18] For a discussion on the sources of the various errors see the second reference of [5].
- [19] J.N. Bahcall *et al.*, *Phys. Rev.* **D54**, 411 (1996).
- [20] D. Majumdar and A. Raychaudhuri, *Phys. Rev.* **D60**, 053001 (1999).
- [21] J.N. Bahcall and E. Lisi, *Phys. Rev.* **D54**, 5417 (1996); S.M. Bilenky and C. Giunti, *Phys. Lett.* **B311**, 179 (1993); *ibid.* **B320**, 323 (1994); G. Fiorentini, M. Lissia, G. Mezzorani, M. Moretti, and D. Vignaud, *Phys. Rev.* **D49**, 6298 (1994); W. Kwong and S.P. Rosen, *ibid.* **D51**, 6159 (1995).
- [22] Y. Fukuda *et al.*, (The Super-Kamiokande collaboration), *Phys. Rev. Lett.* **82**, 1810 (1999).

- [23] J.N. Bahcall and P.I. Krastev, *Phys. Lett.* **B436**, 243 (1998).
- [24] Andre de Gouvea, A. Friedland, and H. Murayama, hep-ph/0002064.
- [25] M.C. Gonzalez-Garcia and C. Peña-Garay, hep-ph/0002186.

Figure Captions

Fig 1. The 90% C.L. allowed region in the $\Delta m^2 - \sin^2(2\theta)$ plane from the analysis of total rates for the Chlorine and Gallium detectors and the 825 day data from SK assuming MSW resonant conversion to (a) sequential neutrinos and (b) sterile neutrinos. The best-fit points are also indicated.

Fig 2. The 95% C.L. allowed region in the $\Delta m^2 - \sin^2(2\theta)$ plane from the 825 day SK recoil electron spectrum data for MSW conversion to (a) sequential neutrinos and (b) sterile neutrinos. The regions enclosed by the contours are *disallowed*. The best-fit points are also indicated.

Fig. 3. The normalized recoil electron energy spectrum for best-fit values of the parameters in (a) the SMA region for the sequential neutrino case, (b) the LMA region for the sequential neutrino case, and (c) both the SMA and LMA regions for the sterile neutrino case. For (a) and (b), the solid (dashed) line is for the low (high) X_B solution. In (c) the solid line is for the low X_B solution in the SMA region while the long (short) dashed line is for the low (high) X_B solution in the LMA region. Also shown are the experimental data points.

Fig. 4. The 90% C.L. allowed region in the $\Delta m^2 - \sin^2(2\theta)$ plane from an analysis of the total rates from the Chlorine and Gallium detectors and the 825 day SK data taken together with the 825 day recoil electron spectrum for (a) sequential neutrinos and (b) sterile neutrinos. The normalization of the ^8B flux is chosen as a free parameter. The best-fit points are also indicated.

Fig. 5. The 90% C.L. allowed region in the $\Delta m^2 - \sin^2(2\theta)$ plane from an analysis of the total rates from the Chlorine and Gallium detectors and the 825 day SK data taken together with the 825 day recoil electron spectrum for (a) sequential neutrinos and (b) sterile neutrinos. Unlike in Fig. 4, the normalization of the ^8B flux is fixed at the SSM value and the correlations between the rates and the recoil energy spectrum due to astrophysical uncertainties in the ^8B flux are included. The best-fit points are also indicated.

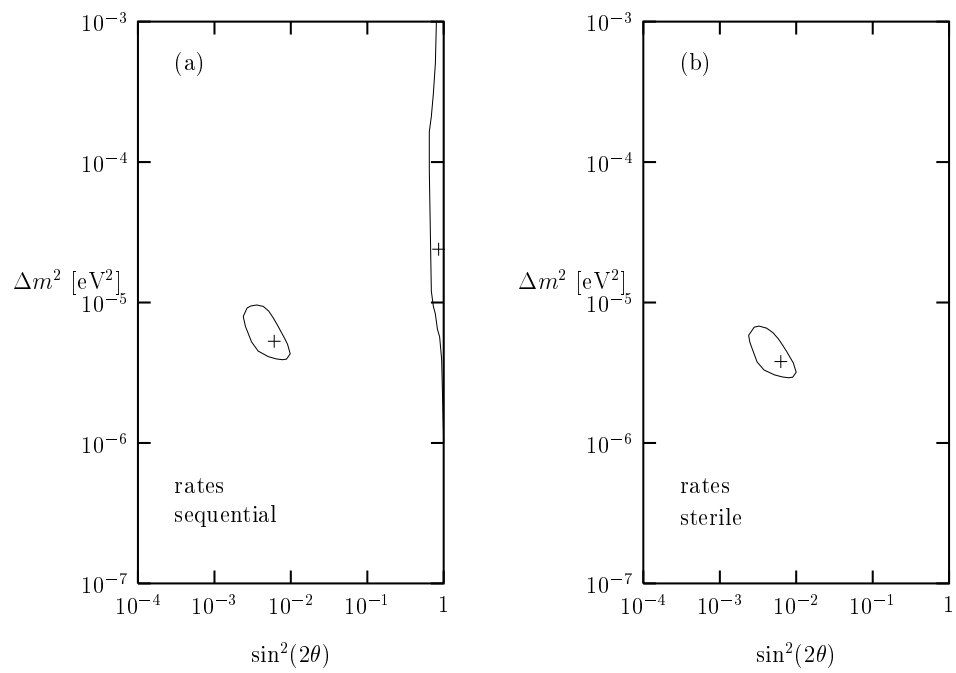


Fig. 1

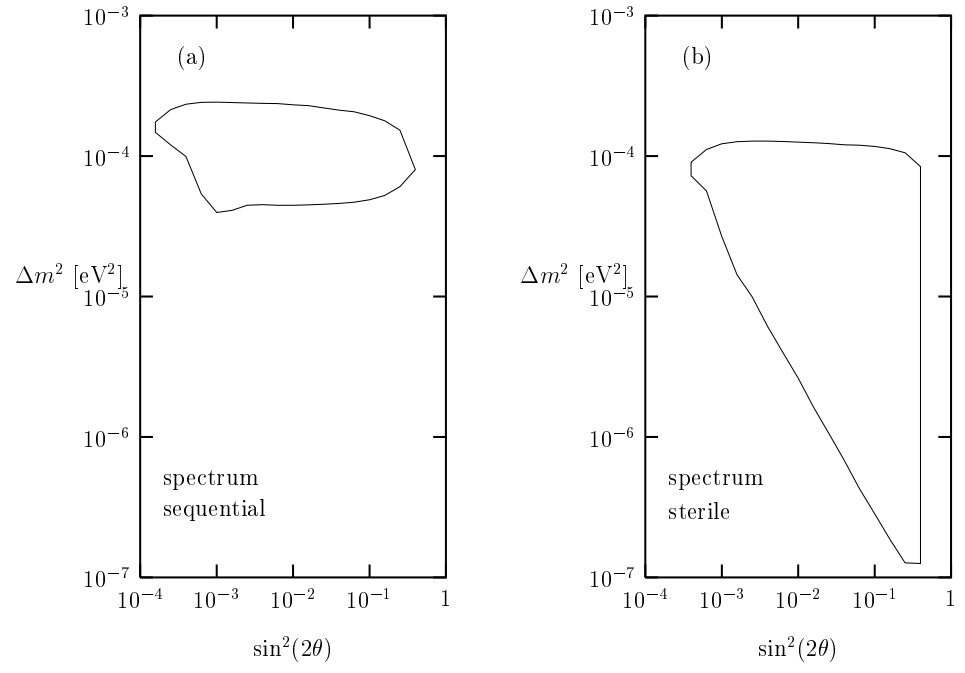


Fig. 2

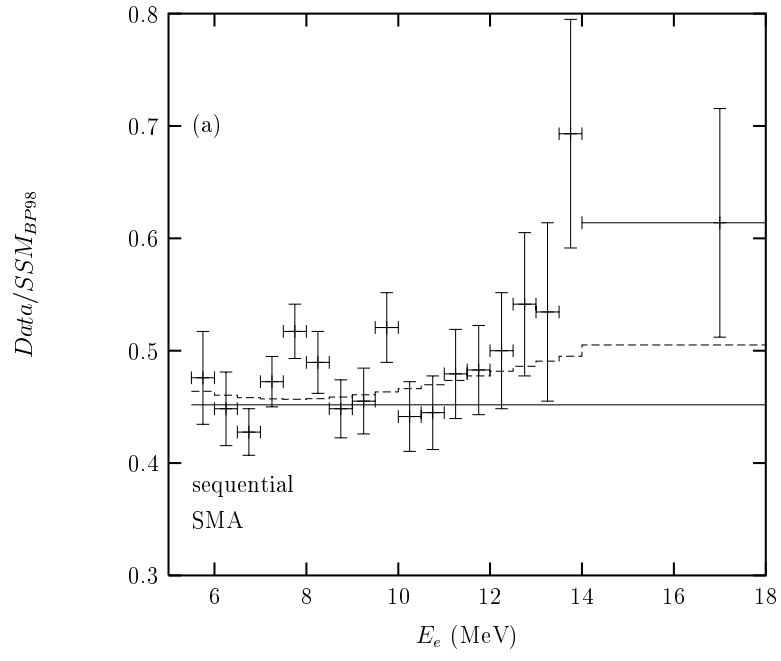


Fig. 3

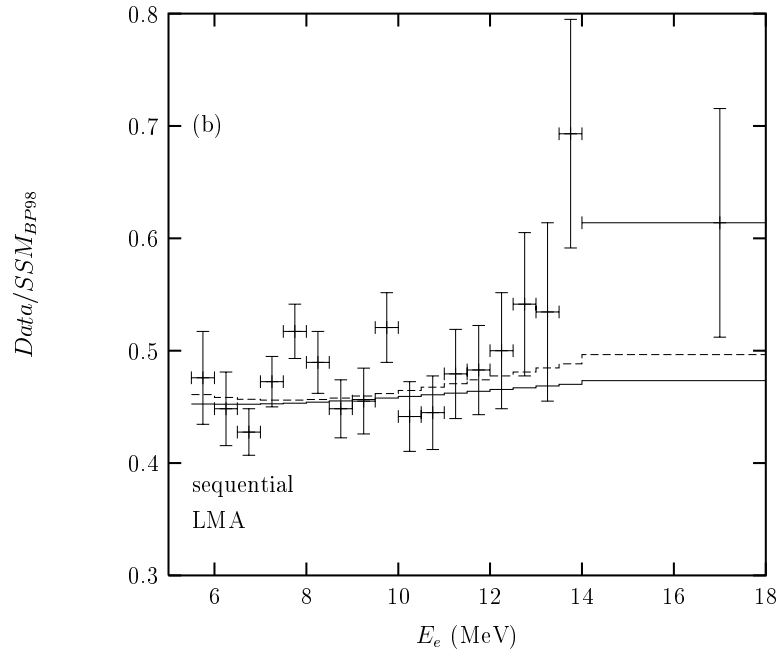


Fig. 3

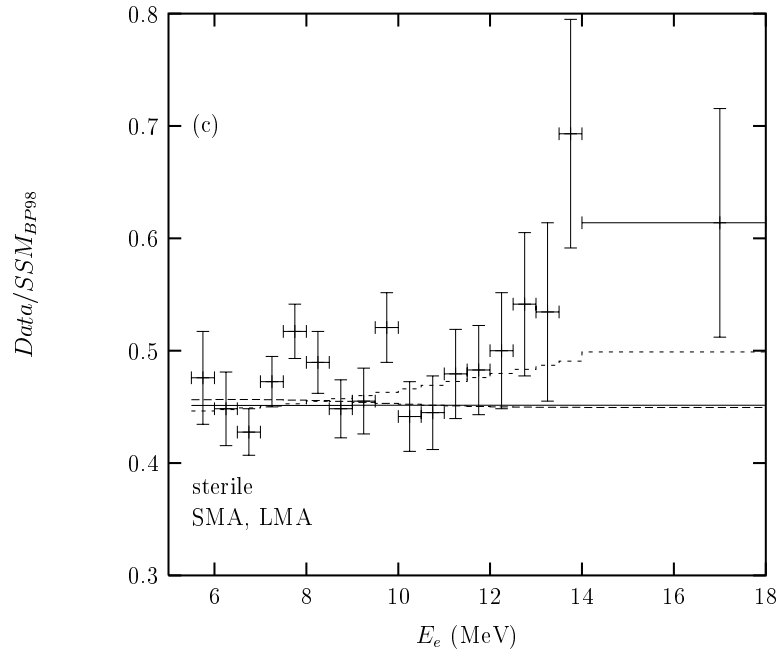


Fig. 3

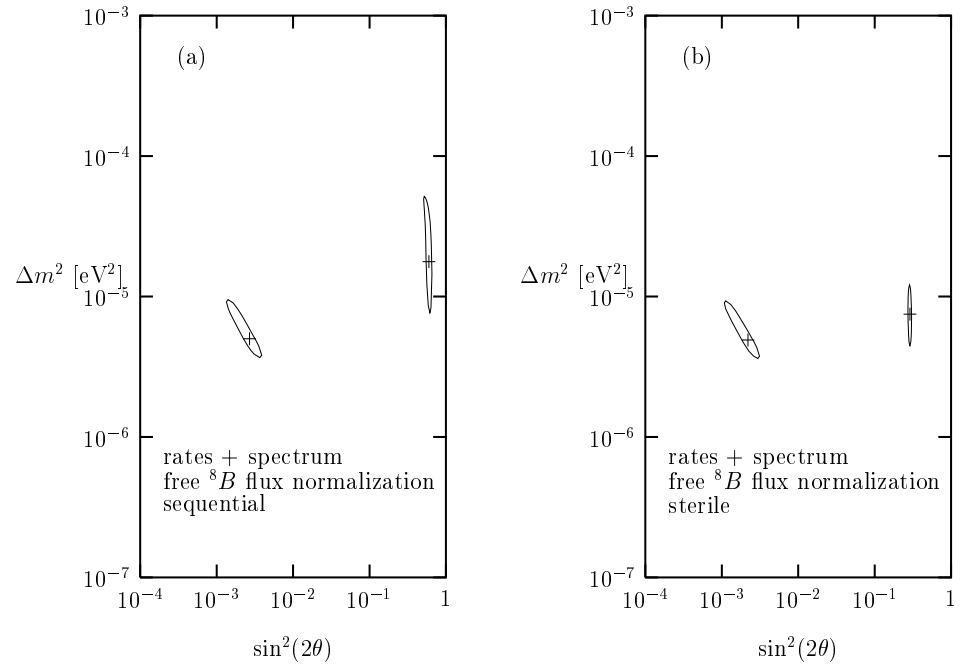


Fig. 4

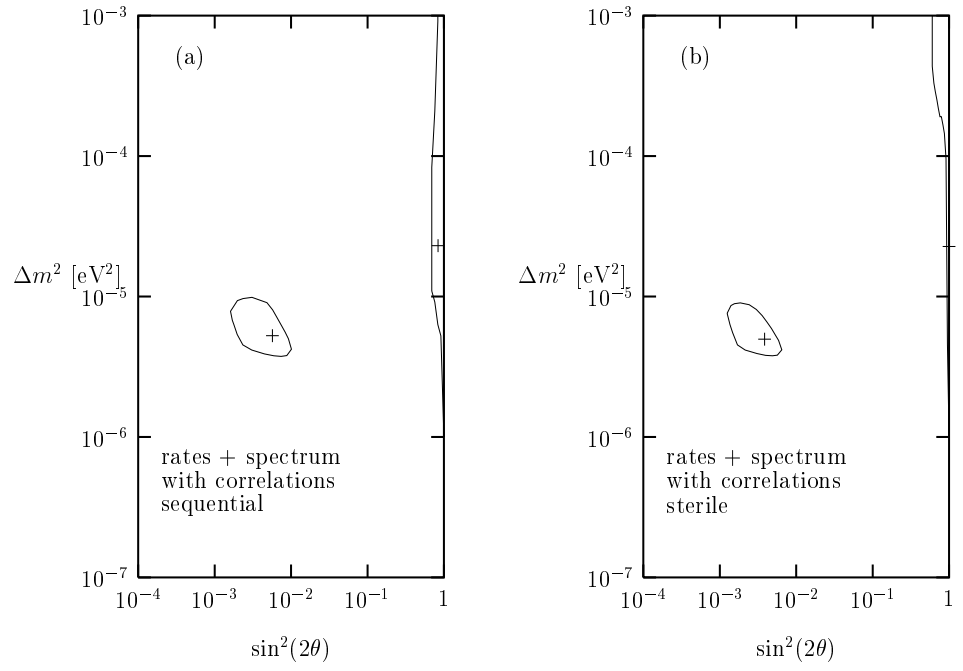


Fig. 5